JACS
JOURNAL OF THE AMERICAN CHEMICAL SOCIETY

COMMUNICATION

pubs.acs.org/JACS

Enhanced Electrocatalytic Reduction of CO_2 with Ternary Ni-Fe_4S_4 and Co-Fe_4S_4-Based Biomimetic Chalcogels

Benjamin D. Yuhas, Chaiya Prasittichai, Joseph T. Hupp, and Mercouri G. Kanatzidis*

Department of Chemistry and Argonne−Northwestern Solar Energy Research (ANSER) Center, Northwestern University, Evanston, Illinois 60208-3113, United States

Supporting Information

ABSTRACT: Enzymes that catalytically transform small molecules such as CO, formate, or protons are naturally composed of transition metal cluster units bound into a larger superstructure. Artificial biomimetic catalysts are often modeled after the active sites but are typically molecular in nature. We present here a series of fully integrated porous materials containing Fe_4S_4 clusters, dubbed "biomimetic chalcogels". We examine the effect of third metal cations on the electrochemical and electrocatalytic properties of the chalcogels. We find that ternary biomimetic chalcogels containing Ni or Co show increased effectiveness in transformations of carbon dioxide and can be thought of as solid-state analogues of NiFe or NiFeS reaction centers in enzymes.

Biomimetic catalysis, which involves the design and development of catalysts that resemble the structure and functionality of natural enzymes, is attracting increased research interest.[1] This is particularly true in the field of solar fuels, where the library of compounds designed to mimic hydrogen- or oxygen-evolving biomolecules is continually growing.[2] The vast majority of biomimetic catalysts are molecular in nature; as such, catalysis is performed in a homogeneous manner. Although homogeneous biomimetic catalysis has been shown to be quite successful for a variety of substrates, many biomimetic catalysts are rapidly deactivated by water and/or oxygen, in contrast to their native counterparts. Homogenous catalysis is further complicated by the nontrivial problem of catalyst retrieval from the reaction solution, as well as separation from the products. For these reasons, any large-scale application involving biomimetic catalysis would benefit from having the active species integrated into a larger matrix, similar to the design found in proteins, with the catalysis proceeding in a heterogeneous fashion.

For heterogeneous catalysis, porous materials are ideal, owing to their high surface areas and low bulk densities. Typical examples, commonly used in industry, are the supported noble metal catalysts,[3] which comprise nanoparticulate, catalytically active metals (e.g., Pt, Rh, Ru) interspersed throughout a porous matrix, such as an oxide aerogel (e.g., SiO_2, TiO_2, Al_2O_3). The well-documented utility of these porous catalysts has inspired efforts to replicate their architecture using biomimetic functionalities or elements of high natural abundance (e.g., Co, Ni, Fe).

Recently, we have reported the synthesis of a new class of porous materials, called chalcogels, which can be functionalized with biomimetic functionalities.[4] These biomimetic chalcogels contain redox-active $[Fe_4S_4]^{2+}$ cluster units linked by $[Sn_2S_6]^{4-}$ cluster units. Chalcogel formation proceeds from a slow, controlled metathesis reaction between the cluster precursors in solution, leading to the bottom-up, polymeric network assembly of redox-active species anchored in a larger semiconducting scaffold. Our chalcogels can be thought of as a hybrid catalyst, combining the features of biomimetic systems with the idealized porous nature of heterogeneous catalysts, all from a one-pot synthesis. This stands in contrast to the typical fabrication of supported noble metal catalysts, which usually require multiple synthetic steps. Our chalcogels are also unique in that the active $[Fe_4S_4]$ subunit is covalently bound to the main-group clusters and fully integrated into the semiconducting chalcogenide matrix, unlike surface-bound metal nanoparticles on an oxide support.

In this Communication, we present a second-generation series of biomimetic chalcogels that contain a third divalent transition metal cation in addition to the $[Fe_4S_4]$ and $[Sn_2S_6]$ clusters. The addition of the third metal allows for the tuning of the $[Fe_4S_4]$ cluster concentration within the gels, which should greatly affect the gels' overall properties. In addition, there could possibly be cooperative effects between the $[Fe_4S_4]$ clusters and the third metal cations, much in the manner of an enzymatic heterometal cluster, such as might be found in hydrogenases or formate dehydrogenase.[5] We focus in this report on the varying electrochemical properties of the three-component chalcogels, hereafter called ternary chalcogels. We show that the addition of transition metals such as Ni^{2+}, Pt^{2+}, Sn^{2+}, and Co^{2+} can result in ternary chalcogels with increased surface area and altered electrochemical properties, such as reduction potential and specific capacitance. Finally, we demonstrate the utility of the ternary chalcogels in the electrocatalytic reduction of carbon dioxide.

Ordinarily, a standard chalcogel is made by combining the precursors $Na_4Sn_2S_6 \cdot 14H_2O$[6] and $(Ph_4P)_2[Fe_4S_4Cl_4]$[7] in mixed solutions of *N,N′*-dimethylformamide (DMF) and formamide. Typically, the concentration ratio of the precursors is near unity, which allows only a narrow synthetic window that will lead to satisfactory gelation. If a third thiophilic metal is added into solution after the $Na_4Sn_2S_6 \cdot 14H_2O$ and $(Ph_4P)_2[Fe_4S_4Cl_4]$ clusters are mixed, gelation can be induced even if the concentration of $[Fe_4S_4]$ relative to $[Sn_2S_6]$ is well below unity (Scheme 1). The ligation of the Fe_4S_4 core with the $[Sn_2S_6]^{4-}$ clusters is similar to that known for molecular analogues investigated previously as bioinorganic model systems of Fe/S

Received: June 27, 2011

 © XXXX American Chemical Society dx.doi.org/10.1021/ja205981v | *J. Am. Chem. Soc.* XXXX, XXX, 000–000

Scheme 1. Synthesis of Ternary Biomimetic Chalcogels

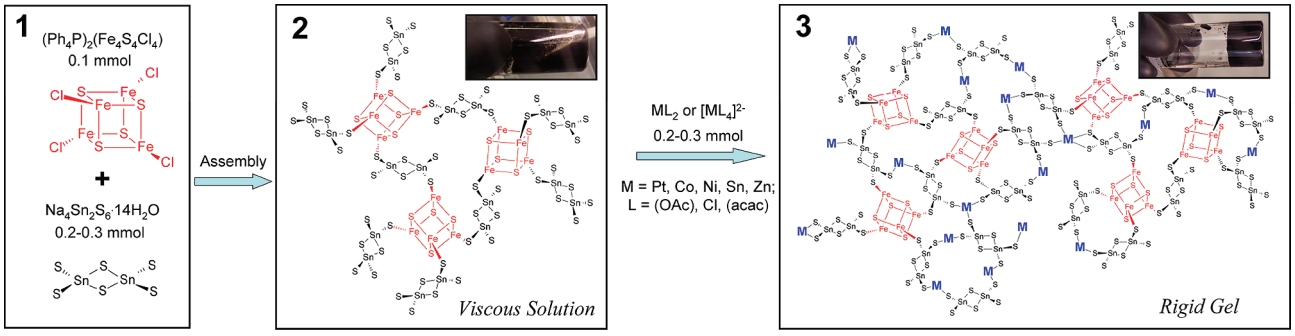

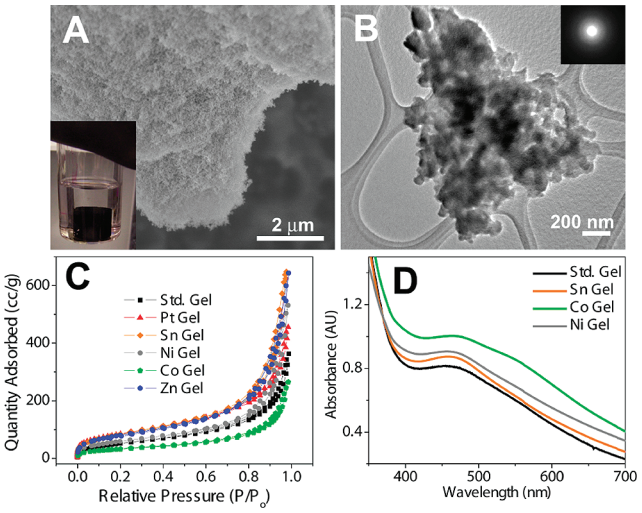

Figure 1. (A,B) SEM and TEM of a Pt−Fe_4S_4−Sn_2S_6 chalcogel. The inset in panel A shows a real-size image of the chalcogel; the inset in panel B is a representative SAED pattern of the chalcogel. All of the ternary chalcogels synthesized are similar in appearance. (C) N_2 adsorption/desorption measurements of standard and ternary chalcogels at 77 K. The measured surface areas range from 110 to 310 m^2/g. (D) UV−vis spectra of chalcogel extrusions with PhSH in DMF.

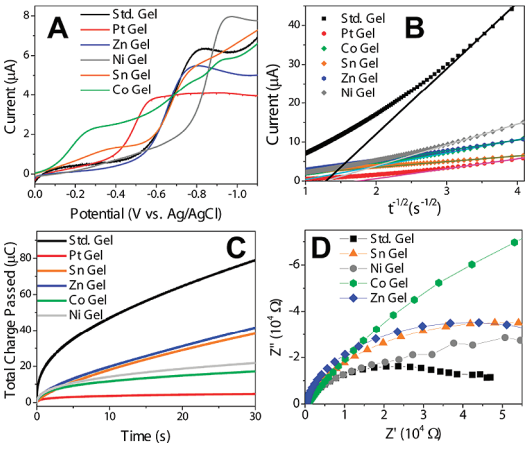

Figure 2. (A) CV curves of standard and ternary chalcogels, recorded at 60 mV/s in MeCN. The currents are normalized to fit on a common scale. (B) Cottrell plots of chalcogel CA curves. The solid lines are fits of the Cottrell equation to the early time points. (C) Chronocoulometry data obtained from integration of the CA plots in panel B. (D) Chalcogel impedance spectra obtained with a constant DC potential of −1000 mV and an amplitude of 10 mV.

proteins.[8] The choice of third metal is quite flexible; we have successfully synthesized biomimetic chalcogels infused with catalytically relevant cations, such as Pt^{2+}, Co^{2+}, and Ni^{2+}, as well as more "inert" cations, such as Zn^{2+} and Sn^{2+}, leading to a chalcogel with the general formula

$$\{M^{2+}_{(2-2x)}[Fe_4S_4]_x[Sn_2S_6]\}$$

Figure 1 displays characteristics of the ternary chalcogels. All chalcogels were found to have similar spongy, amorphous structures (Figure 1A,B). The porosity and surface area of the ternary chalcogels, as determined by N_2 porosimetry (Figure 1C), are similar to those of the standard chalcogels. The estimated surface areas range from 110 to 310 m^2/g (Supporting Information), with the highest surface areas occurring when the third metal is in large excess relative to the $[Fe_4S_4]$ cluster. The addition of the third metal cation does not appear to disrupt or alter the $[Fe_4S_4]$ clusters in any way, as evidenced from gel extrusion experiments (Figure 1D). When a large excess of benzenethiol in DMF is added to the chalcogels, the gels dissolve rapidly, yielding a color and absorption spectrum that are characteristic of the $[Fe_4S_4(SPh)_4]^{2-}$ anion.[7b] Similar spectra are observed in the standard binary chalcogels and the ternary chalcogels.

The standard chalcogels were previously shown to have redox properties that reflected those of the iron−sulfur cluster,[4a] which involve successive one-electron reductions of the $[Fe_4S_4]^{2+}$ core. With the inclusion of the third metal in the ternary chalcogels, the redox properties were examined with cyclic voltammetry (CV) experiments to determine the effect of the third metal. Figure 2A shows the CV curves obtained in the vicinity of the first reduction of various chalcogels. By analogy to the soluble forms, the first and second cathodic waves observed are attributed to the $[Fe_4S_4]^{2+/+}$ and $[Fe_4S_4]^{+/0}$ redox couples, respectively.[7] In some of the ternary chalcogels (Pt, Zn, Sn), the observed reduction potentials are shifted to less negative values. This effect can be explained by thinking of the third metal cation acting as an electron-withdrawing group, which preferentially stabilizes the reduced form of the cluster. It would appear as if the insertion of the third metal were the solid-state analogue of attaching electron-withdrawing moieties onto molecular redox catalysts,[9] allowing for the easier reduction of the $[Fe_4S_4]$ clusters in the gel.

dx.doi.org/10.1021/ja205981v | J. Am. Chem. Soc. XXXX, XXX, 000–000

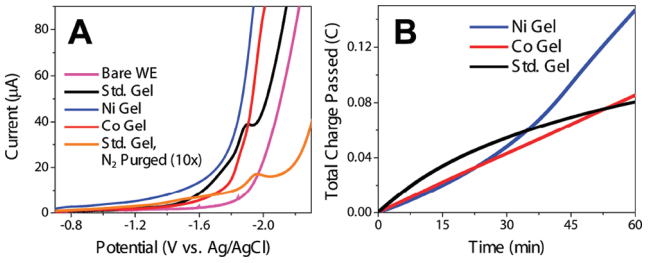

Figure 3. (A) Electrocatalytic reduction of CO_2 in DMF. The supporting electrolyte is 0.1 M $(NBu_4)PF_6$. (B) Chronocoulometry of CO_2 reduction experiments, obtained at −2.0 V.

In addition to the effect on the reduction potential, we probed the effect of the third metals on electron diffusion in the chalcogels. Previous investigations[10] into systems of redox polymers can provide useful insight, for biomimetic chalcogels are similar to redox polymers in that they contain redox-active subunits spatially separated by insulating units with no band structure. The charge-diffusion behavior of the biomimetic chalcogels was examined via chronoamperometry (CA) measurements, in which the current was monitored as a function of time at a constant applied potential of −1.0 V (vs Ag/AgCl). The results are shown in Figure 2B, plotted as current vs $(\text{time})^{-1/2}$. In the case of idealized semi-infinite diffusion conditions, as is expected in solution, the current−time behavior is described by the Cottrell equation:[11]

$$i = \frac{nAFD^{1/2}c}{\pi^{1/2}t^{1/2}}$$

where n is the number of electrons involved in the redox process, A is the electrode area, F is the Faraday constant, c is the molar concentration of electroactive species, and D is the diffusion coefficient. In an idealized transport scenario, a plot of I vs $t^{-1/2}$ would be linear. However, as Figure 2B clearly shows, deviations from Cottrell behavior occur rapidly, with the current at longer times exceeding the values expected on the basis of fitting the early-time behavior. This effect is observed in the Fe_4S_4 chalcogels as well as the ternary M^{2+}/Fe_4S_4 chalcogels.

In the CA experiments, the effect of the third metal is two-fold: First, the absolute currents tend to decrease overall with the addition of the third metal, compared to the standard binary chalcogels. These findings are consistent with the CV experiments and can be explained by the decline in the relative number of redox-active $[Fe_4S_4]$ centers in the gel, which increases the average intercluster distance. Concurrently, this leads to a lowering of the apparent electron diffusion coefficient, as extracted from the early-time components of the CA curves. Further confirmation of this finding is seen in chronocoulometry data (Figure 2C), obtained from the integration of the CA plots. The total amount of the charge passed through the chalcogel is seen to decrease as the ternary metals are integrated into the gel framework. This suggests that charge transport is governed principally by electron hopping between $[Fe_4S_4]$ centers and does not involve the ternary cations. Additional evidence for this is provided by impedance spectroscopy on the chalcogels, shown in Figure 2D. The increase in the semicircle diameter seen in the ternary chalcogels indicates a greater specific resistance in the ternary chalcogels compared to the standard chalcogels. The ternary chalcogels containing Ni and Co also show an increased capacitance compared to the standard chalcogels (Supporting Information). The increased resistance and capacitance values of the ternary chalcogels relative to the standard chalcogels imply that even though the third metal cations can influence the electronic behavior of the neighboring $[Fe_4S_4]$ clusters, they do not themselves participate in charge transport to a major extent.

The high surface area of the chalcogels combined with their ability to store charge effectively makes them ideal candidates for use as electrocatalysts. The $[Fe_4S_4]$ cluster is found frequently in enzymes as an electron-transfer cofactor,[12] while heterometal clusters (such as NiFe clusters) often comprise the enzyme active sites. However, artificial molecular clusters containing the $[Fe_4S_4]$ unit have been shown to have electrocatalytic activity for a variety of substrates,[13] including carbon dioxide. Figure 3 shows the electrocatalytic reduction of CO_2 by the biomimetic chalcogels in DMF. All of the chalcogels show significant current enhancement compared to the bare working electrode, as well as decreased overpotentials. The ternary chalcogels linked with the transition metals Ni and Co are superior to the standard binary chalcogels in terms of overpotential, current, and Tafel slope, enabling CO_2 reduction to begin at approximately −1.7 V, with Tafel slopes of 280 and 235 mV/decade for the Ni- and Co-linked ternary chalcogels, respectively. The onset potential for catalytic reduction is similar to what has been previously observed with other homogeneous catalysts, such as iron porphyrins,[14] nickel(II) cyclams,[15] and molecular $[Fe_4S_4]$ clusters in solution,[13] and is roughly coincident with the potential for the second reduction of the gel-immobilized cluster. When the electrolysis cell is purged with nitrogen, the CV reverts to the previously observed[4a] behavior of the chalcogels, with greatly reduced currents.

We are currently undertaking experiments to analyze the products of the reduction, although this is complicated by the resistive nature of the chalcogels. The high resistances seen in impedance spectroscopy suggest that not all of the $[Fe_4S_4]$ centers may be participating in CO_2 reduction. This is expected since only those clusters immediately adjacent to the electrode surface can be redox activated. As an example, it is seen in Figure 2C that the total charge passed through a standard chalcogel in 30s is approximately 80 μC. Based on elemental data and electrode area, this amount of charge corresponds to only about 2% of the expected charge if all of the $[Fe_4S_4]$ clusters in the gel were reduced. Thus, it is very likely that if the electrode design were to be altered to effectively access the entirety of the gel, the observed catalytic behavior would improve dramatically. (Full calculation details can be found in the Supporting Information.)

Our ternary chalcogels represent a chemically complex and multifunctional material that can be tailored to have high surface areas and desired electrochemical properties, all from a one-pot synthesis driven by a bottom-up assembly process. Much in the manner of placing electron-withdrawing groups on molecular $[Fe_4S_4]$ cluster analogues, the presence of soft metal cations in the biomimetic chalcogels can similarly influence the potential observed for $[Fe_4S_4]$ cluster reduction. The addition of catalytically relevant cations can result in great enhancements to the chalcogels' electrocatalytic ability, as seen in the transformations of CO_2. With the ability to tune the electrochemical properties given by the inclusion of third metals, it is probable that photochemical processes can be similarly enhanced as well, and we are continuing to investigate this area. The ability to tailor the properties of biomimetic chalcogels will provide a rich area

dx.doi.org/10.1021/ja205981v | J. Am. Chem. Soc. XXXX, XXX, 000–000

for research not only into the fundamentals of charge transport in a new porous material but also into the possibility of creating new materials suitable for electrochemical or photodriven catalysis relevant to solar fuels (e.g., the reduction of CO_2) or any other desired substrate.

■ ASSOCIATED CONTENT

Supporting Information. Synthesis and characterization details. This material is available free of charge via the Internet at http://pubs.acs.org.

■ AUTHOR INFORMATION

Corresponding Author
m-kanatzidis@northwestern.edu

■ ACKNOWLEDGMENT

This work was supported as part of the ANSER Center, an Energy Frontier Research Center funded by the U.S. Department of Energy, Office of Science, Office of Basic Energy Sciences, under Award No. DE-SC0001059. Electron Microscopy and Elemental Analysis was performed at the Electron Probe Instrumentation Center at Northwestern University.

■ REFERENCES

(1) (a) Kanan, M. W.; Nocera, D. G. *Science* **2008**, *321*, 1072. (b) Gust, D.; Moore, T. A.; Moore, A. L. *Acc. Chem. Res.* **2009**, *42*, 1890.

(2) (a) Kohl, S. W.; Weiner, L.; Schwartsburd, L.; Konstantinovski, L.; Shimon, L. J. W.; Ben-David, Y.; Iron, M. A.; Milstein, D. *Science* **2009**, *324*, 74. (b) Tard, C.; Liu, X.; Ibrahim, S. K.; Bruschi, M.; De Gioia, L.; Davies, S. C.; Yang, X.; Wang, L.-S.; Sawers, G.; Pickett, C. J. *Nature* **2005**, *433*, 610. (c) Gloaguen, F.; Lawrence, J. D.; Rauchfuss, T. B. *J. Am. Chem. Soc.* **2001**, *123*, 9476.

(3) (a) Grirrane, A.; Corma, A.; Garcia, H. *Science* **2008**, *322*, 1661. (b) Chen, C.; Nan, C.; Wang, D.; Su, Q.; Duan, H.; Liu, X.; Zhang, L.; Chu, D.; Song, W.; Peng, Q.; Li, Y. *Angew. Chem., Int. Ed.* **2011**, *50*, 3725. (c) Joo, S. H.; Park, J. Y.; Tsung, C. K.; Yamada, Y.; Yang, P.; Somorjai, G. A. *Nat. Mater.* **2009**, *8*, 126.

(4) (a) Yuhas, B. D.; Smeigh, A. L.; Samuel, A. P. S.; Shim, Y.; Bag, S.; Douvalis, A. P.; Wasielewski, M. R.; Kanatzidis, M. G. *J. Am. Chem. Soc.* **2011**, *133*, 7252. (b) Bag, S.; Trikalitis, P. N.; Chupas, P. J.; Armatas, G. S.; Kanatzidis, M. G. *Science* **2007**, *317*, 490.

(5) (a) Vincent, K. A.; Parkin, A.; Armstrong, F. A. *Chem. Rev.* **2007**, *107*, 4366. (b) Jeoung, J. H.; Dobbek, H. *Science* **2007**, *318*, 1461.

(6) Krebs, B.; Pohl, S.; Schiwy, W. *Z. Anorg. Allg. Chem.* **1973**, *393*, 241.

(7) (a) Coucouvanis, D.; Kanatzidis, M. G.; Simhon, E.; Baenziger, N. C. *J. Am. Chem. Soc.* **1982**, *104*, 1874. (b) Wong, G. B.; Bobrik, M. A.; Holm, R. H. *Inorg. Chem.* **1978**, *17*, 578.

(8) (a) Rao, P. V.; Holm, R. H. *Chem. Rev.* **2004**, *104*, 527. (b) Kanatzidis, M.; Ryan, M.; Coucouvanis, D.; Simopoulos, A.; Kostikas, A. *Inorg. Chem.* **1983**, *22*, 179. (c) Kanatzidis, M. G.; Salifoglou, A.; Coucouvanis, D. *Inorg. Chem.* **1986**, *25*, 2460–2468. (d) Coucouvanis, D.; Kanatzidis, M. G.; Dunham, W. R.; Hagen, W. R. *J. Am. Chem. Soc.* **1984**, *106*, 7998–7999. (e) Kanatzidis, M. G.; Coucouvanis, D.; Simopoulos, A.; Kostikas, A.; Papaefthymiou, V. *J. Am. Chem. Soc.* **1985**, *107*, 4925–4935.

(9) Zhou, C.; Raebiger, J. W.; Segal, B. M.; Holm, R. H. *Inorg. Chim. Acta* **2000**, *300*, 892.

(10) (a) Daum, P.; Lenhard, J. R.; Rolison, D.; Murray, R. W. *J. Am. Chem. Soc.* **1980**, *102*, 4649. (b) Mao, F.; Mano, N.; Heller, A. *J. Am. Chem. Soc.* **2003**, *125*, 4951.

(11) Bard, A. J.; Faulkner, L. R. *Electrochemical Methods: Fundamentals and Applications*; Wiley: New York, 1980; p 143.

(12) Surerus, K. K.; Chen, M.; van der Zwaan, J. W.; Rusnak, F. M.; Kolk, M.; Duin, E. C.; Albracht, S. P. J.; Muenck, E. *Biochemistry* **1994**, *33*, 4980.

(13) (a) Tezuka, M.; Yajima, T.; Tsuchiya, A.; Matsumoto, Y.; Uchida, Y.; Hidai, M. *J. Am. Chem. Soc.* **1982**, *104*, 6834. (b) Tanaka, K.; Imasaka, Y.; Tanaka, M.; Honjo, M.; Tanaka, T. *J. Am. Chem. Soc.* **1982**, *104*, 4258.

(14) Hammouche, M.; Lexa, D.; Momenteau, M.; Saveant, J.-M. *J. Am. Chem. Soc.* **1991**, *113*, 8455.

(15) (a) Collin, J. P.; Jouaiti, A.; Sauvage, J. P. *Inorg. Chem.* **1988**, *27*, 1986. (b) Benson, E. E.; Kubiak, C. P.; Sathrum, A. J.; Smieja, J. M. *Chem. Soc. Rev.* **2009**, *38*, 98.